Mathematics

https://www.aimspress.com/journal/Math

AIMS Mathematics, 10(3): 4899–4914.
DOI:10.3934/math.2025224
Received: 05 December 2024
Revised: 18 February 2025
Accepted: 26 February 2025
Published: 06 March 2025

Research article

An efficient numerical method for highly oscillatory logarithmic-algebraic singular integrals

SAIRA[1], **Wenxiu Ma**[1,2,3,4,*] **and Suliman Khan**[5]

[1] School of mathematical sciences, Zhejiang Normal University, Jinhua, 321004, China
[2] Department of Mathematics, King Abdulaziz University, Jeddah, 21589, Saudi Arabia
[3] Department of Mathematics and Statistics, University of South Florida, Tampa, FL 33620-5700, USA
[4] School of Mathematical and Statistical Sciences, North-West University, Mafikeng Campus, Private Bag X2046, Mmabatho 2735, South Africa
[5] State Key Laboratory of Mechanics and Control for Aerospace Structures, College of Aerospace Engineering, Nanjing University of Aeronautics and Astronautics, Nanjing, 210016, China

* **Correspondence:** Email: mawx@cas.usf.edu.

Abstract: This paper discussed the numerical evaluation of highly oscillatory integrals involving logarithmic and algebraic singularities. For an analytic function in a sufficiently large region containing $[a, b]$, the integral was transformed into the sum of two line integrals where the integrands did not oscillate and decay exponentially. Thus, to approximate the line integrals, generalized Gauss-Laguerre quadrature and logarithmic Gauss-Laguerre quadrature were applied. The error bound and numerical results demonstrated that the proposed method efficiently obtained high-precision results even for high oscillations.

Keywords: algebraic singularities; logarithmic singularity; high oscillations; analytic function; Gauss-Laguerre quadrature
Mathematics Subject Classification: 30E20, 32A55, 42B20, 45E05

1. Introduction

Many scientific and engineering phenomena can be studied and modeled using integral equations. They provide a versatile framework for modeling complex systems, solving boundary value problems, analyzing signals, studying fluid dynamics and solid mechanics, addressing inverse problems, and developing numerical methods [1–8]. Such integral equations can also possess integrals involving logarithmic or algebraic singularities.

This paper discusses the numerical computation of the following highly oscillatory integral involving both algebraic and logarithmic singularities

$$I[f(\alpha,\beta,s)] = \int_a^b \frac{[\ln(x-a)\ln(b-x)]^s f(x) e^{i\omega x}}{(x-a)^\alpha (b-x)^\beta \prod_{k=1}^n (x-\tau_k)^{\gamma_k}} dx, \quad s \in \{0,1\}, \tag{1.1}$$

where $f(x)$ is a non-oscillatory, real-valued function on $[a,b]$, $\omega \gg 1$ is the frequency, $-\infty < a < b < \infty$, $\alpha,\beta < 1, \gamma_k \leq 1$, and $a < \tau_k < b$. Nevertheless, these integrals play a significant role in quantum mechanics, wave propagation, fluid dynamics, and electromagnetic theory, where they are used to formulate mixed boundary value problems. For $\alpha = \beta = s = \gamma_k = 0$, there are sufficient methods such as the Filon method, Clenshaw-Curtis method, asymptotic method, Levin method, steepest descent method, and meshless method to solve this integral [9–12]. In addition, for $\gamma_k = s = 0$, a vast number of numerical methods have been proposed, some of which are the Filon method, modified Clenshaw-Curtis method, Levin method, and steepest descent method [13–15].

In [16], Kang et al. presented two quadrature methods to solve the singularly oscillatory integral for $\gamma_k = s = 0$ over the interval $[0,b]$. A two-point Taylor polynomial was employed to perform the two-point Taylor interpolation. Their approach involves utilizing the Taylor polynomial of the function f at $x = 0$, and converting the integral into two integrals based on the additivity of the integration interval. By using the generalized Gaussian-Laguerre quadrature rule and the Cauchy residue theorem, one integral can be computed efficiently. Some special functions can be used to calculate the other integrals. In the paper [17], the author presented fast and accurate numerical schemes for evaluating highly oscillatory integrals with weak and Cauchy singularities. The authors in [18] implemented the meshless collocation method based on the Levin approach to treat the Cauchy-type and logarithmic singularities. The proposed algorithms compute the integrals accurately for large-scale data points and high frequency.

In [19], the high order Clenshaw-Curtis-Filon methods based on special Hermite interpolation polynomial $P_{N+2r}, r \in \{0,1,2\}$ in Clenshaw-Curtis points $N+1$ are constructed for calculating many classes of oscillatory integrals with algebraic or logarithmic singularities. Some stable recurrence relations are further used to calculate the obtained modified moments accurately and efficiently. The accuracy of the methods is claimed to improve for fixed N when ω or r increases. As for some classical quadrature methods, such as Gaussian quadrature or any quadrature method that uses polynomial interpolation, a substantial number of quadrature points is required. In the case of large ω, the numerical evaluation by such quadratures can be very challenging. In [20], the authors implemented the Clenshaw-Curtis quadrature convergence rate for Jacobi weights given for functions with algebraic endpoint singularities using the aliasing asymptotics on the coefficients of the Chebyshev expansions. For this type of function, the optimal error bound is obtained based on a newly designed symmetric Jacobi weight. In this instance, the Clenshaw-Curtis quadrature is exponentially convergent for a newly constructed Jacobi weight. Using few numerical examples, the theoretical results are verified.

However, in [21] the authors implemented an interpolatory quadrature rule to compute the Cauchy-type and logarithmic singularities. In [22], the author presented a method for fast evaluation of highly oscillatory Fourier-type integrals with Jacobi-type singularities by the Gauss-Laguerre rule. The author asserts that these integrals can be computed stably and efficiently with a moderate to large frequency, and this claim has been verified through a few numerical experiments. Moreover, Chen [23] has computed (1.1), where $s = 0$. The author provided a numerical method based on the steepest descent method for an analytic function. The general Gauss-Laguerre quadrature rule is implemented to compute the line integrals containing non-oscillatory integrands. To prove the validity of the given convergence rate of the problem, several numerical examples are also provided. Kurtoğlu et al. [24] presented a problem for $\gamma_k = 0$, which was solved by the steepest descent method. This method consists of three-term recursion coefficients for orthogonal polynomials w.r.t Gautschi's weight functions and appropriate Gauss quadrature rules.

One spectra computation method for the highly oscillatory integral equation with an algebraic and logarithmic singularity is proposed by Gao [25]. In this work, the integral equations are converted into algebraic eigenvalue problems using the finite section method. This conversion leads to an infinite coefficient matrix whose entries are bivariate highly oscillatory singular integrals. By simplifying the double integral, they get an explicit expression. An augmented Levin method is presented in [26] for the computation of oscillatory integrals with stationary points and an algebraically or logarithmically singular kernel. In conjunction with the truncated singular value decomposition, sparse and fast spectral methods are applied to convert the original Levin ordinary differential equation(ODE) into an augmented ODE system.

Considering the wide range of applications of these types of integrals, it is of great interest to develop an algorithm for computing these integrals numerically that is both fast and accurate. The existing numerical methods will not be able to solve integrals of (1.1) type due to the existence of logarithmic and algebraic singularities. We are primarily concerned with providing a fast algorithm for the efficient computation of these integrals. Hence, this paper provides a reliable numerical method for solving such integrals where $\gamma_k \neq 0$ and $s = 1$. Based on analytic continuation, the proposed method consists of converting highly oscillatory integrals into the problem of integrating a sum of two line integrals which contain the integrand that does not oscillate and decays exponentially. In addition, the N-point generalized Gauss-Laguerre quadrature rule and N-point logarithmic Gauss-Laguerre quadrature rule are used to compute these line integrals. It is claimed that for larger values of ω, precise approximated results can be obtained for fixed N. Furthermore, the numerical examples provide sufficient evidence that the proposed numerical method produces highly accurate results, regardless of singularities or frequency.

This paper is organized as follows: Section 1 introduces the problem along with the literature review. Section 2 explains the main methodology for computing the integral (1.1). An error bound is provided in Section 3, while numerical examples are presented in Section 4 to demonstrate the authenticity of the proposed method. Finally, the paper is concluded with a few remarks in Section 5.

2. Numerical scheme to compute the integral (1.1)

This section provides the numerical method depending on contour integration on the complex plane for (1.1). In light of the significant results of Cauchy's theorem from complex analysis, Cauchy's theorem states that the value of a line integral of an analytic function along a path between two points in the complex plane does not depend on the exact path taken [27], and we prove the following theorem:

Theorem 1. *Let's consider a function $f(z)$, which is an analytic in the upper half-strip of the complex plane $a \leq \Re(z) \leq b$ and $\Im(z) \geq 0$, and satisfies that*

$$\int_a^b \frac{|\ln(z+iR-a)||\ln(b-z-iR)||f(z+iR)|}{|(z+iR-a)^{\alpha}||(b-z-iR)^{\beta}||\prod_{k=1}^{n}(z+iR-\tau_k)^{\gamma_k}|}dz \leq MR^{\alpha+\beta}e^{\omega_0 R}, \quad 0<\omega_0<\omega,$$

for M and ω_0 constants, then the integral (1.1) can be transformed as:

$$I[f(\alpha,\beta,1)]=\begin{cases}-(-\frac{i}{\omega})^{1-\beta}e^{i\omega b}\int_0^{\infty}\frac{\ln(b+\frac{it}{\omega}-a)\ln(-\frac{it}{\omega})f(b+\frac{it}{\omega})t^{-\beta}e^{-t}}{(b+\frac{it}{\omega}-a)^{\alpha}\prod_{k=1}^{n}(b+\frac{it}{\omega}-\tau_k)^{\gamma_k}}dt+(\frac{i}{\omega})^{1-\alpha}e^{i\omega a}\int_0^{\infty}\frac{\ln(b-\frac{it}{\omega}-a)\ln(\frac{it}{\omega})f(a+\frac{it}{\omega})t^{-\alpha}e^{-t}}{(b-\frac{it}{\omega}-a)^{\beta}\prod_{k=1}^{n}(a+\frac{it}{\omega}-\tau_k)^{\gamma_k}}dt\\+\sum_{k=1}^{p}\frac{i\pi\ln(\tau_k-a)\ln(b-\tau_k)f(\tau_k)e^{i\omega(\tau_k)}}{(\tau_k-a)^{\alpha}(b-\tau_k)^{\beta}\prod_{j=1}^{k-1}(\tau_k-\tau_j)^{\gamma_j}\prod_{j=k+1}^{n}(\tau_k-\tau_j)^{\gamma_j}},\ when\ \gamma_k=1,(k=1,\cdots,p),\ j\neq k;\\-(-\frac{i}{\omega})^{1-\beta}e^{i\omega b}\int_0^{\infty}\frac{\ln(b+\frac{it}{\omega}-a)\ln(-\frac{it}{\omega})f(b+\frac{it}{\omega})t^{-\beta}e^{-t}}{(b+\frac{it}{\omega}-a)^{\alpha}\prod_{k=1}^{n}(b+\frac{it}{\omega}-\tau_k)^{\gamma_k}}dt+(\frac{i}{\omega})^{1-\alpha}e^{i\omega a}\int_0^{\infty}\frac{\ln(b-\frac{it}{\omega}-a)\ln(\frac{it}{\omega})f(a+\frac{it}{\omega})t^{-\alpha}e^{-t}}{(b-\frac{it}{\omega}-a)^{\beta}\prod_{k=1}^{n}(a+\frac{it}{\omega}-\tau_k)^{\gamma_k}}dt,\\ when\quad \gamma_k<1,(k=1,\cdots,n).\end{cases} \tag{2.1}$$

Proof. Since $\frac{\ln(z-a)\ln(b-z)f(z)e^{i\omega z}}{(z-a)^{\alpha}(b-z)^{\beta}\prod_{k=1}^{n}(z-\tau_k)^{\gamma_k}}$ is analytic in the upper half-strip of complex plane D, where region D is enclosed by the curves $\Gamma_1,\Gamma_2,\Gamma_3,\Gamma_4,\Gamma_7,\sum_{k=1}^{n}\Gamma_{5,k},\sum_{k=1}^{n}\Gamma_{6,k}$ as shown in the Figure 1. Following the Cauchy's theorem, we obtain

$$I[f(\alpha,\beta,1)]=\int_{\Gamma_1+\Gamma_2+\Gamma_3+\Gamma_4+\Gamma_7+\sum_{k=1}^{n}\Gamma_{5,k}+\sum_{k=1}^{n}\Gamma_{6,k}}\frac{\ln(z-a)\ln(b-z)f(z)e^{i\omega z}}{(z-a)^{\alpha}(b-z)^{\beta}\prod_{k=1}^{n}(z-\tau_k)^{\gamma_k}}dz=0. \tag{2.2}$$

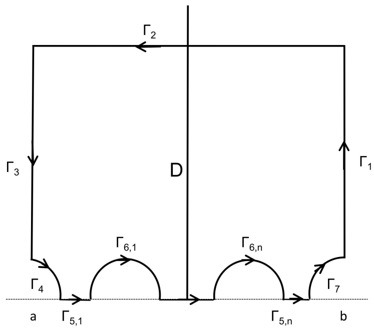

Figure 1. Integration path for integral (1.1).

For $\int_{\Gamma_1}$, let $z=b+ip, p\in[R,r]$, where R is a large number and r is a small number. Then, we get

$$\begin{aligned}\int_{\Gamma_1}&=i\int_r^R\frac{\ln(b+ip-a)\ln(-ip)f(b+ip)e^{i\omega(b+ip)}}{(b+ip-a)^{\alpha}(-ip)^{\beta}\prod_{k=1}^{n}(b+ip-\tau_k)^{\gamma_k}}dp\\&=(-i)^{1-\beta}e^{i\omega b}\int_r^R\frac{\ln(b+ip-a)\ln(-ip)f(b+ip)e^{-\omega p}}{(b+ip-a)^{\alpha}(p)^{\beta}\prod_{k=1}^{n}(b+ip-\tau_k)^{\gamma_k}}dp\\&=(-\frac{i}{\omega})^{1-\beta}e^{i\omega b}\int_r^R\frac{\ln(b+\frac{it}{\omega}-a)\ln(-\frac{it}{\omega})f(b+\frac{it}{\omega})t^{-\beta}e^{-t}}{(b+\frac{it}{\omega}-a)^{\alpha}\prod_{k=1}^{n}(b+\frac{it}{\omega}-\tau_k)^{\gamma_k}}dt.\end{aligned}$$

Similarly, for $\int_{\Gamma_3}, z=a+ip, p\in[R,r]$, we have

$$\begin{aligned}\int_{\Gamma_3}&=-i\int_r^R\frac{\ln(ip)\ln(b-ip-a)f(a+ip)e^{i\omega(a+ip)}}{(ip)^{\alpha}(b-ip-a)^{\beta}\prod_{k=1}^{n}(a+ip-\tau_k)^{\gamma_k}}dp\\&=-(\frac{i}{\omega})^{1-\alpha}e^{i\omega a}\int_r^R\frac{\ln(\frac{it}{\omega})\ln(b-\frac{it}{\omega}-a)f(a+\frac{it}{\omega})t^{-\alpha}e^{-t}}{(b-\frac{it}{\omega}-a)^{\beta}\prod_{k=1}^{n}(a+\frac{it}{\omega}-\tau_k)^{\gamma_k}}dt.\end{aligned}$$

Now for $\int_{\Gamma_2}, z = x + iR$, we obtain

$$\begin{aligned}\Big|\int_{\Gamma_2}\Big| &= \Big|\int_a^b \frac{\ln(x+iR-a)\ln(b-x-iR)f(x+iR)e^{i\omega(x+iR)}}{(x+iR-a)^{\alpha}(b-x-iR)^{\beta}\prod_{k=1}^{n}(x+iR-\tau_k)^{\gamma_k}}dx\Big|\\ &\le e^{-\omega R}\int_a^b\Big|\frac{\ln(x+iR-a)\ln(b-x-iR)f(x+iR)e^{i\omega x}}{(x+iR-a)^{\alpha}(b-x-iR)^{\beta}\prod_{k=1}^{n}(x+iR-\tau_k)^{\gamma_k}}\Big|dx\\ &\le Me^{-(\omega-\omega_0)R}\to 0,\quad \text{as}\quad R\to\infty.\end{aligned}$$

For $\int_{\Gamma_4}, z = a + re^{i\theta}$, we achieve

$$\begin{aligned}\int_{\Gamma_4} &= \int_0^{\pi/2}\frac{\ln(re^{i\theta})\ln(b-a-re^{i\theta})f(a+re^{i\theta})e^{i\omega a}e^{i\omega re^{i\theta}}}{(re^{i\theta})^{\alpha}(b-a-re^{i\theta})^{\beta}\prod_{k=1}^{n}(a+re^{i\theta}-\tau_k)^{\gamma_k}}ire^{i\theta}d\theta\\ &\le r^{1+\alpha}\Big|\int_0^{\pi/2}\frac{|\ln(re^{i\theta})||\ln(b-a-re^{i\theta})||f(a+re^{i\theta})|}{(b-a-re^{i\theta})^{\beta}\prod_{k=1}^{n}(a+re^{i\theta}-\tau_k)^{\gamma_k}}d\theta\Big|\\ &\to 0,\quad \text{as}\quad r\to 0,\end{aligned}$$

following the same steps for Γ_7, $\Gamma_7 \to 0$, as $r \to 0$.

The paths $\int_{\Gamma_{6,k}}(k = 1, \cdots, n)$, when $z = \tau_k + re^{i\theta}, 0 \le \theta \leqslant \pi$, become

$$\int_{\Gamma_{6,k}} = \begin{cases}\int_0^{\pi}\frac{\ln(\tau_k+re^{i\theta}-a)\ln(b-\tau_k-re^{i\theta})f(\tau_k+re^{i\theta})e^{i\omega(\tau_k+re^{i\theta})}}{(\tau_k+re^{i\theta}-a)^{\alpha}(b-\tau_k-re^{i\theta})^{\beta}\prod_{j=1}^{k-1}(\tau_k+re^{i\theta}-\tau_j)^{\gamma_j}\prod_{j=k+1}^{n}(\tau_k+re^{i\theta}-\tau_j)^{\gamma_j}}ire^{i\theta}d\theta,\\ -\sum_{k=1}^{p}\frac{i\pi\ln(\tau_k-a)\ln(b-\tau_k)f(\tau_k)e^{i\omega(\tau_k)}}{(\tau_k-a)^{\alpha}(b-\tau_k)^{\beta}\prod_{j=1}^{k-1}(\tau_k-\tau_j)^{\gamma_j}\prod_{j=k+1}^{n}(\tau_k-\tau_j)^{\gamma_j}},\quad \text{when}\quad \gamma_k = 1;\\ 0,\quad \text{when}\quad \gamma_k < 1.\end{cases}$$

Then, to calculate the $I[f(\alpha,\beta,1)]$, (2.2) leads to

$$I[f(\alpha,\beta,1)] = \sum_{k=1}^{n}\int_{\Gamma_{5,k}} = -\int_{\Gamma_1}-\int_{\Gamma_2}-\int_{\Gamma_3}-\int_{\Gamma_4}-\int_{\Gamma_7}-\sum_{k=1}^{n}\int_{\Gamma_{6,k}}, \tag{2.3}$$

which completes the proof. □

Using the Gautschi [28] analysis, the complex logarithmic functions are transformed as

$$\ln(\frac{i}{\omega}t) = (\frac{\pi}{2}i - \ln(\omega) - 1 + t) - (t - 1 - \ln(t)),\quad \ln(\frac{-i}{\omega}t) = (-\frac{\pi}{2}i - \ln(\omega) - 1 + t) - (t - 1 - \ln(t)).$$

By substituting the above logarithmic functions into two line integrals $\bar{I}[f(\beta)]$ and $\bar{I}[f(\alpha)]$, we get

$$\begin{aligned}\bar{I}[f(\beta)] &= -(-\frac{i}{\omega})^{1-\beta}e^{i\omega b}\int_0^{\infty}\frac{\ln(b+\frac{it}{\omega}-a)\ln(-\frac{it}{\omega})f(b+\frac{it}{\omega})t^{-\beta}e^{-t}}{(b+\frac{it}{\omega}-a)^{\alpha}\prod_{k=1}^{n}(b+\frac{it}{\omega}-\tau_k)^{\gamma_k}}dt\\ &= -(-\frac{i}{\omega})^{1-\beta}e^{i\omega b}\Big(\int_0^{\infty}\frac{\ln(b+\frac{it}{\omega}-a)(-\frac{\pi}{2}i-\ln(\omega)-1+t)f(b+\frac{it}{\omega})t^{-\beta}e^{-t}}{(b+\frac{it}{\omega}-a)^{\alpha}\prod_{k=1}^{n}(b+\frac{it}{\omega}-\tau_k)^{\gamma_k}}dt\\ &\quad -\int_0^{\infty}\frac{\ln(b+\frac{it}{\omega}-a)(t-1-\ln(t))f(b+\frac{it}{\omega})t^{-\beta}e^{-t}}{(b+\frac{it}{\omega}-a)^{\alpha}\prod_{k=1}^{n}(b+\frac{it}{\omega}-\tau_k)^{\gamma_k}}dt\Big).\end{aligned} \tag{2.4}$$

$$
\begin{aligned}
\bar{I}[f(\alpha)] =&(\frac{i}{\omega})^{1-\alpha}e^{i\omega a}\int_0^{\infty}\frac{\ln(b-\frac{it}{\omega}-a)\ln(\frac{it}{\omega})f(a+\frac{it}{\omega})t^{-\alpha}e^{-t}}{(b-\frac{it}{\omega}-a)^{\beta}\prod_{k=1}^{n}(a+\frac{it}{\omega}-\tau_k)^{\gamma_k}}dt\\
=&(\frac{i}{\omega})^{1-\alpha}e^{i\omega a}\Bigg(\int_0^{\infty}\frac{\ln(b-\frac{it}{\omega}-a)(\frac{\pi}{2}i-\ln(\omega)-1+t)f(a+\frac{it}{\omega})t^{-\alpha}e^{-t}}{(b-\frac{it}{\omega}-a)^{\beta}\prod_{k=1}^{n}(a+\frac{it}{\omega}-\tau_k)^{\gamma_k}}dt\\
&-\int_0^{\infty}\frac{\ln(b-\frac{it}{\omega}-a)(t-1-\ln(t))f(a+\frac{it}{\omega})t^{-\alpha}e^{-t}}{(b-\frac{it}{\omega}-a)^{\beta}\prod_{k=1}^{n}(a+\frac{it}{\omega}-\tau_k)^{\gamma_k}}dt\Bigg).
\end{aligned}
\tag{2.5}
$$

Combining (2.4) and (2.5), (2.1) leads to the following:

$$
I[f(\alpha,\beta,1)]=\begin{cases}
-(-\frac{i}{\omega})^{1-\beta}e^{i\omega b}\Big(\int_0^{\infty}\frac{\ln(b+\frac{it}{\omega}-a)(-\frac{\pi}{2}i-\ln(\omega)-1+t)f(b+\frac{it}{\omega})t^{-\beta}e^{-t}}{(b+\frac{it}{\omega}-a)^{\alpha}\prod_{k=1}^{n}(b+\frac{it}{\omega}-\tau_k)^{\gamma_k}}dt-\int_0^{\infty}\frac{\ln(b+\frac{it}{\omega}-a)(t-1-\ln(t))f(b+\frac{it}{\omega})t^{-\beta}e^{-t}}{(b+\frac{it}{\omega}-a)^{\alpha}\prod_{k=1}^{n}(b+\frac{it}{\omega}-\tau_k)^{\gamma_k}}dt\Big)\\
+(\frac{i}{\omega})^{1-\alpha}e^{i\omega a}\Big(\int_0^{\infty}\frac{\ln(b-\frac{it}{\omega}-a)(\frac{\pi}{2}i-\ln(\omega)-1+t)f(a+\frac{it}{\omega})t^{-\alpha}e^{-t}}{(b-\frac{it}{\omega}-a)^{\beta}\prod_{k=1}^{n}(a+\frac{it}{\omega}-\tau_k)^{\gamma_k}}dt-\int_0^{\infty}\frac{\ln(b-\frac{it}{\omega}-a)(t-1-\ln(t))f(a+\frac{it}{\omega})t^{-\alpha}e^{-t}}{(b-\frac{it}{\omega}-a)^{\beta}\prod_{k=1}^{n}(a+\frac{it}{\omega}-\tau_k)^{\gamma_k}}dt\Big)\\
+\frac{i\pi\ln(\tau_k-a)\ln(b-\tau_k)f(\tau_k)e^{i\omega(\tau_k)}}{(\tau_k-a)^{\alpha}(b-\tau_k)^{\beta}\prod_{j=1}^{k-1}(\tau_k-\tau_j)^{\gamma_j}\prod_{j=\kappa+1}^{n}(\tau_k-\tau_j)^{\gamma_j}}, \quad \text{when} \quad \gamma_{\kappa}=1,(k=1,\cdots,p);\\
-(-\frac{i}{\omega})^{1-\beta}e^{i\omega b}\Big(\int_0^{\infty}\frac{\ln(b+\frac{it}{\omega}-a)(-\frac{\pi}{2}i-\ln(\omega)-1+t)f(b+\frac{it}{\omega})t^{-\beta}e^{-t}}{(b+\frac{it}{\omega}-a)^{\alpha}\prod_{k=1}^{n}(b+\frac{it}{\omega}-\tau_k)^{\gamma_k}}dt-\int_0^{\infty}\frac{\ln(b+\frac{it}{\omega}-a)(t-1-\ln(t))f(b+\frac{it}{\omega})t^{-\beta}e^{-t}}{(b+\frac{it}{\omega}-a)^{\alpha}\prod_{k=1}^{n}(b+\frac{it}{\omega}-\tau_k)^{\gamma_k}}dt\Big)\\
+(\frac{i}{\omega})^{1-\alpha}e^{i\omega a}\Big(\int_0^{\infty}\frac{\ln(b-\frac{it}{\omega}-a)(\frac{\pi}{2}i-\ln(\omega)-1+t)f(a+\frac{it}{\omega})t^{-\alpha}e^{-t}}{(b-\frac{it}{\omega}-a)^{\beta}\prod_{k=1}^{n}(a+\frac{it}{\omega}-\tau_k)^{\gamma_k}}dt-\int_0^{\infty}\frac{\ln(b-\frac{it}{\omega}-a)(t-1-\ln(t))f(a+\frac{it}{\omega})t^{-\alpha}e^{-t}}{(b-\frac{it}{\omega}-a)^{\beta}\prod_{k=1}^{n}(a+\frac{it}{\omega}-\tau_k)^{\gamma_k}}dt\Big),\\
\text{when} \quad \gamma_k<1,(k=1,\cdots,n).
\end{cases}
\tag{2.6}
$$

Consider $\{t_m^{\beta},w_m^{\beta}\}_{m=1}^{N}$ and $\{t_m^{\alpha},w_m^{\alpha}\}_{m=1}^{N}$ nodes and weights of the N-point generalized Gauss-Laguerre quadrature rule w.r.t weight functions $t^{-\beta}e^{-t}$ and $t^{-\alpha}e^{-t}$, respectively. Meanwhile, $\{t_m^{\beta,l},w_m^{\beta,l}\}_{m=1}^{N}$ and $\{t_m^{\alpha,l},w_m^{\alpha,l}\}_{m=1}^{N}$ denote the nodes and weights of the N-point logarithmic-Gauss-Laguerre quadrature rule w.r.t weight functions $(t-1-\ln(t))t^{-\beta}e^{-t}$ and $(t-1-\ln(t))t^{-\alpha}e^{-t}$, respectively. Thus, $\bar{I}[f(\beta)]$ and $\bar{I}[f(\alpha)]$ can be computed as follows:

$$
\begin{aligned}
\bar{Q}_N[f(\beta)] =&-(-\frac{i}{\omega})^{1-\beta}e^{i\omega b}\Bigg(\sum_{m=1}^{N}\frac{\ln(b+\frac{it_m^{\beta}}{\omega}-a)(-\frac{\pi}{2}i-\ln(\omega)-1+t_m^{\beta})f(b+\frac{it_m^{\beta}}{\omega})}{(b+\frac{it_m^{\beta}}{\omega}-a)^{\alpha}\prod_{k=1}^{n}(b+\frac{it_m^{\beta}}{\omega}-\tau_k)^{\gamma_k}}w_m^{\beta}\\
&-\sum_{m=1}^{N}\frac{\ln(b+\frac{it_m^{\beta,l}}{\omega}-a)f(b+\frac{it_m^{\beta,l}}{\omega})}{(b+\frac{it_m^{\beta,l}}{\omega}-a)^{\alpha}\prod_{k=1}^{n}(b+\frac{it_m^{\beta,l}}{\omega}-\tau_k)^{\gamma_k}}w_m^{\beta,l}\Bigg).
\end{aligned}
\tag{2.7}
$$

$$
\begin{aligned}
\bar{Q}_N[f(\alpha)] =&(\frac{i}{\omega})^{1-\alpha}e^{i\omega a}\Bigg(\sum_{m=1}^{N}\frac{\ln(b-\frac{it_m^{\alpha}}{\omega}-a)(\frac{\pi}{2}i-\ln(\omega)-1+t_m^{\alpha})f(a+\frac{it_m^{\alpha}}{\omega})}{(b-\frac{it}{\omega}-a)^{\beta}\prod_{k=1}^{n}(a+\frac{it_m^{\alpha}}{\omega}-\tau_k)^{\gamma_k}}w_m^{\alpha}\\
&-\sum_{m=1}^{N}\frac{\ln(b-\frac{it_m^{\alpha,l}}{\omega}-a)f(a+\frac{it_m^{\alpha,l}}{\omega})}{(b-\frac{it_m^{\alpha,l}}{\omega}-a)^{\beta}\prod_{k=1}^{n}(a+\frac{it_m^{\alpha,l}}{\omega}-\tau_k)^{\gamma_k}}w_m^{\alpha,l}\Bigg).
\end{aligned}
\tag{2.8}
$$

Based on (2.7) and (2.8), the numerical method to compute (2.6) is defined as

$$Q_N[f(\alpha,\beta,1)]=\begin{cases}-(-\frac{i}{\omega})^{1-\beta}e^{i\omega b}\left(\sum_{m=1}^{N}\frac{\ln(b+\frac{it_m^{\beta}}{\omega}-a)(-\frac{\pi}{2}i-\ln(\omega)-1+t_m^{\beta})f(b+\frac{it_m^{\beta}}{\omega})}{(b+\frac{it_m^{\beta}}{\omega}-a)^{\alpha}\prod_{k=1}^{n}(b+\frac{it_m^{\beta}}{\omega}-\tau_k)^{\gamma_k}}w_m^{\beta}-\sum_{m=1}^{N}\frac{\ln(b+\frac{it_m^{\beta,l}}{\omega}-a)f(b+\frac{it_m^{\beta,l}}{\omega})}{(b+\frac{it_m^{\beta,l}}{\omega}-a)^{\alpha}\prod_{k=1}^{n}(b+\frac{it_m^{\beta,l}}{\omega}-\tau_k)^{\gamma_k}}w_m^{\beta,l}\right)\\ +(\frac{i}{\omega})^{1-\alpha}e^{i\omega a}\left(\sum_{m=1}^{N}\frac{\ln(b-\frac{it_m^{\alpha}}{\omega}-a)(\frac{\pi}{2}i-\ln(\omega)-1+t_m^{\alpha})f(a+\frac{it_m^{\alpha}}{\omega})}{(b-\frac{it}{\omega}-a)^{\beta}\prod_{k=1}^{n}(a+\frac{it_m^{\alpha}}{\omega}-\tau_k)^{\gamma_k}}w_m^{\alpha}-\sum_{m=1}^{N}\frac{\ln(b-\frac{it_m^{\alpha,l}}{\omega}-a)f(a+\frac{it_m^{\alpha,l}}{\omega})}{(b-\frac{it_m^{\alpha,l}}{\omega}-a)^{\beta}\prod_{k=1}^{n}(a+\frac{it_m^{\alpha,l}}{\omega}-\tau_k)^{\gamma_k}}w_m^{\alpha,l}\right)\\ +\sum_{k=1}^{p}\frac{i\pi\ln(\tau_k-a)\ln(b-\tau_k)f(\tau_k)e^{i\omega(\tau_k)}}{(\tau_k-a)^{\alpha}(b-\tau_k)^{\beta}\prod_{j=1}^{k-1}(\tau_k-\tau_j)^{\gamma_j}\prod_{j=k+1}^{n}(\tau_k-\tau_j)^{\gamma_j}},\ \text{when } \gamma_k=1,(k=1,\cdots,p);\\ -(-\frac{i}{\omega})^{1-\beta}e^{i\omega b}\left(\sum_{m=1}^{N}\frac{\ln(b+\frac{it_m^{\beta}}{\omega}-a)(-\frac{\pi}{2}i-\ln(\omega)-1+t_m^{\beta})f(b+\frac{it_m^{\beta}}{\omega})}{(b+\frac{it_m^{\beta}}{\omega}-a)^{\alpha}\prod_{k=1}^{n}(b+\frac{it_m^{\beta}}{\omega}-\tau_k)^{\gamma_k}}w_m^{\beta}-\sum_{m=1}^{N}\frac{\ln(b+\frac{it_m^{\beta,l}}{\omega}-a)f(b+\frac{it_m^{\beta,l}}{\omega})}{(b+\frac{it_m^{\beta,l}}{\omega}-a)^{\alpha}\prod_{k=1}^{n}(b+\frac{it_m^{\beta,l}}{\omega}-\tau_k)^{\gamma_k}}w_m^{\beta,l}\right)\\ +(\frac{i}{\omega})^{1-\alpha}e^{i\omega a}\left(\sum_{m=1}^{N}\frac{\ln(b-\frac{it_m^{\alpha}}{\omega}-a)(\frac{\pi}{2}i-\ln(\omega)-1+t_m^{\alpha})f(a+\frac{it_m^{\alpha}}{\omega})}{(b-\frac{it}{\omega}-a)^{\beta}\prod_{k=1}^{n}(a+\frac{it_m^{\alpha}}{\omega}-\tau_k)^{\gamma_k}}w_m^{\alpha}-\sum_{m=1}^{N}\frac{\ln(b-\frac{it_m^{\alpha,l}}{\omega}-a)f(a+\frac{it_m^{\alpha,l}}{\omega})}{(b-\frac{it_m^{\alpha,l}}{\omega}-a)^{\beta}\prod_{k=1}^{n}(a+\frac{it_m^{\alpha,l}}{\omega}-\tau_k)^{\gamma_k}}w_m^{\alpha,l}\right),\\ \text{when}\quad \gamma_k<1,(k=1,\cdots,n).\end{cases}\tag{2.9}$$

In case $s=0$,

$$Q_N[f(\alpha,\beta,0)]=\begin{cases}-(-\frac{i}{\omega})^{1-\beta}e^{i\omega b}\left(\sum_{m=1}^{N}\frac{f(b+\frac{it_m^{\beta}}{\omega})}{(b+\frac{it_m^{\beta}}{\omega}-a)^{\alpha}\prod_{k=1}^{n}(b+\frac{it_m^{\beta}}{\omega}-\tau_k)^{\gamma_k}}w_m^{\beta}\right)+(\frac{i}{\omega})^{1-\alpha}e^{i\omega a}\left(\sum_{m=1}^{N}\frac{f(a+\frac{it_m^{\alpha}}{\omega})}{(b-\frac{it}{\omega}-a)^{\beta}\prod_{k=1}^{n}(a+\frac{it_m^{\alpha}}{\omega}-\tau_k)^{\gamma_k}}w_m^{\alpha}\right)\\ +\sum_{k=1}^{p}\frac{i\pi f(\tau_k)e^{i\omega(\tau_k)}}{(\tau_\kappa-a)^{\alpha}(b-\tau_\kappa)^{\beta}\prod_{j=1}^{\kappa-1}(\tau_k-\tau_j)^{\gamma_j}\prod_{j=\kappa+1}^{n}(\tau_k-\tau_j)^{\gamma_j}},\quad \text{when}\quad \gamma_\kappa=1,(k=1,\cdots,n);\\ -(-\frac{i}{\omega})^{1-\beta}e^{i\omega b}\left(\sum_{m=1}^{N}\frac{f(b+\frac{it_m^{\beta}}{\omega})}{(b+\frac{it_m^{\beta}}{\omega}-a)^{\alpha}\prod_{k=1}^{n}(b+\frac{it_m^{\beta}}{\omega}-\tau_k)^{\gamma_k}}w_m^{\beta}\right)+(\frac{i}{\omega})^{1-\alpha}e^{i\omega a}\left(\sum_{m=1}^{N}\frac{f(a+\frac{it_m^{\alpha}}{\omega})}{(b-\frac{it}{\omega}-a)^{\beta}\prod_{k=1}^{n}(a+\frac{it_m^{\alpha}}{\omega}-\tau_k)^{\gamma_k}}w_m^{\alpha}\right),\\ \text{when}\quad \gamma_k<1,(k=1,\cdots,p),\end{cases}$$

and the results $Q_N[f(\alpha,\beta,0)]$ to compute $I[f(\alpha,\beta,0)]$ are consistent with those given in [23].

3. Error analysis

Theorem 2. *Let $f(z)$ be an analytic and non-oscillatory function in the upper half-strip of the complex plane $a \le \Re(z) \le b$ and $\Im(z) \ge 0$, then the error of the numerical method (2.9) for integral (1.1) can be defined as*

$$|I[f(\alpha,\beta,1)]-Q_N[f(\alpha,\beta,1)]| = O(\omega^{-2N-min(\alpha,\beta)}),\quad \omega\to\infty.\tag{3.1}$$

Proof. The error formula of the N-point generalized Gauss-Laguerre quadrature rule to the integral $\int_0^{+\infty} f(x)x^{\nu}e^{-x}dx, \nu > -1$ [29] is given as

$$E_N = \frac{N!\Gamma(N+\nu+1)}{(2N)!}f^{(2N)}(\zeta),\quad 0<\zeta<+\infty.\tag{3.2}$$

Using (3.2) yields that

$$\begin{aligned}
&\Bigg|\int_0^{\infty}\frac{\ln(b+\frac{it}{\omega}-a)(-\frac{\pi}{2}i-\ln(\omega)-1+t)f(b+\frac{it}{\omega})t^{-\beta}e^{-t}}{(b+\frac{it}{\omega}-a)^{\alpha}\prod_{k=1}^{n}(b+\frac{it}{\omega}-\tau_k)^{\gamma_k}}dt\\
&-\sum_{m=1}^{N}\frac{\ln(b+\frac{it_m^{\beta}}{\omega}-a)(-\frac{\pi}{2}i-\ln(\omega)-1+t_m^{\beta})f(b+\frac{it_m^{\beta}}{\omega})}{(b+\frac{it_m^{\beta}}{\omega}-a)^{\alpha}\prod_{k=1}^{n}(b+\frac{it_m^{\beta}}{\omega}-\tau_k)^{\gamma_k}}w_m^{\beta}\Bigg|\\
=&\left|\frac{N!\Gamma(N-\beta+1)}{(2N)!}\frac{d^{2N}}{dt^{2N}}\left(\frac{\ln(b+\frac{it}{\omega}-a)(-\frac{\pi}{2}i-\ln(\omega)-1+t)f(b+\frac{it}{\omega})}{(b+\frac{it}{\omega}-a)^{\alpha}\prod_{k=1}^{n}(b+\frac{it}{\omega}-\tau_k)^{\gamma_k}}\right)\right|_{t=\zeta_1}\\
=&O(\omega^{-2N}).
\end{aligned}\tag{3.3}$$

Similarly, by employing the N-point generalized Gauss-Laguerre quadrature rule for the integral $\int_0^{+\infty} f(x)(x-1-\log(x))x^{\nu}e^{-x}dx, \nu > -1$ [30], the error formula can be considered as

$$E_N = \frac{h_N}{k_N^2(2N)!}f^{(2N)}(\zeta), \quad 0 < \zeta < +\infty. \tag{3.4}$$

Using (3.4), we get

$$\begin{aligned}
&\Bigg|\int_0^{\infty}\frac{\ln(b+\frac{it}{\omega}-a)(t-1-\ln(t))f(b+\frac{it}{\omega})t^{-\beta}e^{-t}}{(b+\frac{it}{\omega}-a)^{\alpha}\prod_{k=1}^{n}(b+\frac{it}{\omega}-\tau_k)^{\gamma_k}}-\sum_{m=1}^{N}\frac{\ln(b+\frac{it_m^{\beta,l}}{\omega}-a)f(b+\frac{it_m^{\beta,l}}{\omega})}{(b+\frac{it_m^{\beta,l}}{\omega}-a)^{\alpha}\prod_{k=1}^{n}(b+\frac{it_m^{\beta,l}}{\omega}-\tau_k)^{\gamma_k}}w_m^{\beta,l}\Bigg|\\
=&\left|\frac{h_N}{k_N^2(2N)!}\frac{d^{2N}}{dt^{2N}}\left(\frac{\ln(b+\frac{it}{\omega}-a)f(b+\frac{it}{\omega})}{(b+\frac{it}{\omega}-a)^{\alpha}\prod_{k=1}^{n}(b+\frac{it}{\omega}-\tau_k)^{\gamma_k}}\right)\right|_{t=\zeta_2}\\
=&O(\omega^{-2N}).
\end{aligned}\tag{3.5}$$

A combination of (3.3) and (3.5), derives the result

$$|\bar{I}[f(\beta)] - \bar{Q}_N[f(\beta)]| = O(\omega^{-2N-\beta}), \tag{3.6}$$

and by using a similar method, we have

$$|\bar{I}[f(\alpha] - \bar{Q}_N[f(\alpha)]| = O(\omega^{-2N-\alpha}). \tag{3.7}$$

Thus, (3.6) and (3.7) leads to the following:

$$|I[f(\alpha,\beta,1)] - Q_N[f(\alpha,\beta,1)]| = O(\omega^{-2N-min(\alpha,\beta)}), \quad \omega \to \infty. \tag{3.8}$$

□

4. Numerical examples

This section provides numerical examples illustrating how the proposed method produces more precise results. The values considered to be exact are calculated by taking sufficiently large values of N for the quadrature rule. Moreover, in the following examples, absolute error and relative error are calculated as $AE_N = |I[f(\alpha,\beta,1)] - Q_N[f(\alpha,\beta,1)]|$ and $RE_N = |\frac{I[f(\alpha,\beta,1)]-Q_N[f(\alpha,\beta,1)]}{I[f(\alpha,\beta,1)]}|$, respectively. It is apparent in Tables 1 to 9 that the given approach produces higher accuracy results with a fixed N as the frequency ω increases or fixed ω with N increasing. In Examples 3 to 5, Figures 2, 4, and 6 illustrate the absolute error as well as Figures 3, 5, and 7 verify the error bound provided in Theorem 2. Table 8 shows that for $N = 5$, more accurate results can be achieved than those of the Clenshaw-Curtis-Filon method given in [14] for $s = \gamma_k = 0$. Moreover, Table 9 compares the proposed method and the high order Clenshaw-Curtis-Filon method [19] based on Hermite interpolation $P_{N+2r}, r \in \{0, 1, 2\}$. All numerical examples are tested in Matlab R2023a. The experiments were performed on a computer with an Intel Core i7 1.99 GHz processor and 8 GB of RAM.

Example 1. *Consider the following highly oscillatory logarithmic-algebraic singular integral:*

$$I[f(\alpha,\beta,1)] = \int_0^1 \frac{\ln(x-a)\ln(b-x)f(x)e^{i\omega x}}{(x-a)^{0.3}(b-x)^{0.4}(x-0.5)^{\gamma}}dx. \tag{4.1}$$

Tables 1 and 2 exhibit the absolute error for (4.1) computed by the proposed method, where $f(x) = sin(x)$ and e^x are considered for $\gamma = 1$ and 0.25. These tables show that higher accuracy results can be obtained for different values of N and ω.

Table 1. The absolute error for the integral (4.1), where $f(x) = e^x$.

		$\gamma = 1$			
ω	N=1	N=2	N=3	N=4	N=5
16	2.5019×10^{-02}	1.9170×10^{-04}	1.1352×10^{-04}	1.3324×10^{-05}	1.4109×10^{-06}
32	4.4982×10^{-03}	7.7524×10^{-05}	2.4969×10^{-06}	8.6891×10^{-08}	9.6777×10^{-10}
64	5.1965×10^{-04}	1.9425×10^{-06}	2.1171×10^{-08}	3.9205×10^{-10}	9.1229×10^{-12}
100	4.0881×10^{-04}	5.9939×10^{-07}	1.8939×10^{-09}	1.0857×10^{-11}	9.0151×10^{-14}
		$\gamma = 0.25$			
16	4.4961×10^{-03}	1.5955×10^{-04}	9.8546×10^{-06}	1.4312×10^{-07}	1.0497×10^{-07}
32	1.4454×10^{-03}	1.0176×10^{-05}	1.06649×10^{-07}	2.8443×10^{-10}	2.3419×10^{-10}
64	2.6104×10^{-04}	5.1483×10^{-07}	2.0873×10^{-09}	1.6374×10^{-11}	1.4127×10^{-13}
100	6.9661×10^{-05}	5.3669×10^{-08}	7.8543×10^{-11}	2.0247×10^{-13}	4.8027×10^{-16}

Table 2. The absolute error for the integral (4.1), where $f(x) = sin(x)$.

		$\gamma = 1$			
ω	N=1	N=2	N=3	N=4	N=5
16	8.7971×10^{-03}	6.4991×10^{-05}	3.2995×10^{-05}	3.8779×10^{-06}	4.0988×10^{-07}
32	1.6240×10^{-03}	2.2830×10^{-05}	7.2783×10^{-07}	2.5293×10^{-08}	2.8115×10^{-10}
64	2.2926×10^{-04}	5.7784×10^{-07}	6.1712×10^{-09}	1.1405×10^{-11}	2.6534×10^{-12}
100	1.3814×10^{-04}	1.7704×10^{-07}	5.5228×10^{-10}	3.1597×10^{-12}	2.5797×10^{-14}
		$\gamma = 0.25$			
ω	N=1	N=2	N=3	N=4	N=5
16	1.0387×10^{-02}	1.4169×10^{-04}	3.9576×10^{-06}	7.3553×10^{-07}	1.9663×10^{-08}
32	3.3818×10^{-03}	1.1911×10^{-05}	2.2383×10^{-07}	7.4183×10^{-09}	1.4550×10^{-10}
64	1.1523×10^{-03}	7.3880×10^{-07}	2.5575×10^{-09}	3.6767×10^{-11}	7.6360×10^{-13}
100	5.4517×10^{-04}	2.3058×10^{-07}	4.1691×10^{-10}	1.7234×10^{-12}	1.2080×10^{-14}

Example 2. *We compute the following highly oscillatory logarithmic-algebraic singular integral:*

$$I[f(\alpha,\beta,1)] = \int_{-1}^{2} \frac{\ln(x-a)\ln(b-x)f(x)e^{i\omega x}}{(x-a)^{0.25}(b-x)^{0.67}(x-0.5)^{\gamma}}dx. \tag{4.2}$$

Tables 3 and 4 demonstrate the absolute error for (4.2) computed by the proposed method, where $f(x) = sin(x)$ and e^x are considered for $\gamma = 1$ and 0.25. The results in these tables illustrate that the absolute error decays for different values of N and ω.

Table 3. The absolute error for the integral (4.2), where $f(x) = e^x$.

		$\gamma = 1$			
ω	N=1	N=2	N=3	N=4	N=5
16	5.4109×10^{-02}	5.0436×10^{-05}	3.5121×10^{-07}	9.1072×10^{-09}	2.3272×10^{-10}
32	2.0124×10^{-02}	2.9934×10^{-06}	8.8245×10^{-09}	5.3313×10^{-11}	3.7356×10^{-13}
64	8.0763×10^{-03}	3.9809×10^{-07}	1.7532×10^{-10}	3.2672×10^{-13}	3.9721×10^{-15}
100	4.4738×10^{-03}	9.7296×10^{-08}	1.1176×10^{-11}	1.6758×10^{-14}	1.0741×10^{-14}
		$\gamma = 0.25$			
ω	N=1	N=2	N=3	N=4	N=5
16	1.3568×10^{-01}	2.2617×10^{-04}	2.8969×10^{-07}	3.6345×10^{-10}	7.8237×10^{-12}
32	5.3236×10^{-02}	2.2695×10^{-05}	7.2418×10^{-09}	1.6402×10^{-12}	1.0049×10^{-14}
64	2.0644×10^{-02}	2.2039×10^{-06}	1.7434×10^{-10}	1.2810×10^{-14}	5.0243×10^{-15}
100	1.1347×10^{-02}	4.9752×10^{-07}	1.6120×10^{-11}	1.4459×10^{-14}	1.0805×10^{-14}

Table 4. The absolute error for the integral (4.2), where $f(x) = sin(x)$.

		$\gamma = 1$			
ω	N=1	N=2	N=3	N=4	N=5
16	1.0120×10^{-02}	1.1040×10^{-05}	1.1431×10^{-07}	2.6130×10^{-09}	6.7293×10^{-11}
32	4.0522×10^{-03}	1.5639×10^{-07}	3.1632×10^{-09}	1.5340×10^{-11}	1.1108×10^{-13}
64	1.5929×10^{-03}	7.0363×10^{-08}	6.6182×10^{-11}	9.4826×10^{-14}	6.2803×10^{-16}
100	8.7682×10^{-04}	1.8344×10^{-08}	4.9202×10^{-12}	3.6146×10^{-15}	8.8991×10^{-16}
		$\gamma = 0.25$			
ω	N=1	N=2	N=3	N=4	N=5
16	8.4422×10^{-03}	1.4257×10^{-05}	3.1224×10^{-08}	9.1619×10^{-11}	1.8926×10^{-12}
32	2.3132×10^{-03}	9.9918×10^{-07}	8.4400×10^{-10}	6.2828×10^{-13}	4.2130×10^{-15}
64	1.1195×10^{-03}	1.1932×10^{-07}	2.0359×10^{-11}	5.6217×10^{-15}	5.0243×10^{-15}
100	5.9877×10^{-04}	2.6306×10^{-08}	1.9069×10^{-12}	1.8971×10^{-15}	6.2804×10^{-16}

Example 3. *For the following highly oscillatory logarithmic-algebraic singular integral*

$$I[f(\alpha,\beta,1)] = \int_{-1}^{1} \frac{\ln(x-a)\ln(b-x)f(x)e^{i\omega x}}{(x-a)^{0.5}(b-x)^{0.25}(x-0.1)^{\gamma}}dx, \tag{4.3}$$

Table 5 illustrates the absolute error of the integral (4.3) for $f(x) = e^x$ and $\gamma = 1$, computed by the proposed method. Figure 2 exhibits the absolute error, while Figure 3 shows the scaled absolute error *for (4.3) for different values of N and ω from* 10 *to* 1000*. From Figure 2, it is evident that absolute error decays as ω increases.*

Table 5. The absolute error for the integral (4.3), where $f(x) = e^x$ and $\gamma = 1$.

ω	N=1	N=2	N=3	N=4	N=5
16	4.7363×10^{-03}	9.7077×10^{-06}	5.6466×10^{-07}	2.2761×10^{-08}	1.4088×10^{-09}
32	9.2576×10^{-04}	1.3682×10^{-06}	1.1814×10^{-08}	2.2426×10^{-10}	5.1658×10^{-12}
64	1.6992×10^{-04}	1.3318×10^{-07}	1.2655×10^{-10}	6.0465×10^{-13}	5.5132×10^{-15}
100	3.8099×10^{-04}	6.9435×10^{-09}	2.2250×10^{-11}	4.0757×10^{-14}	1.3878×10^{-16}

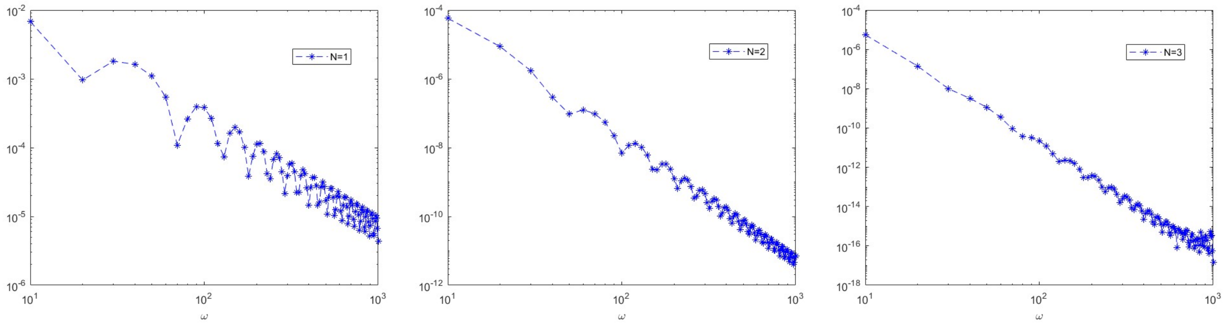

Figure 2. Absolute error for the integral (4.3), where $f(x) = e^x$ and N=1,2,3.

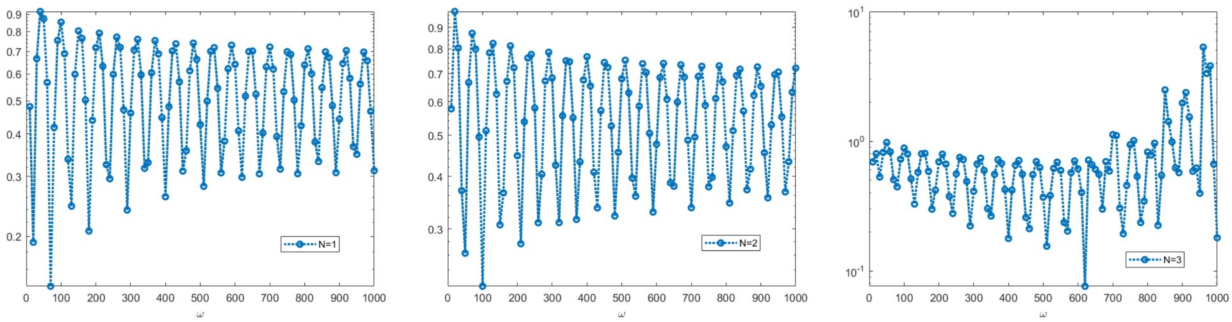

Figure 3. Absolute error scaled by (3.1) for the integral (4.3), where $f(x) = e^x$ and N=1,2,3.

Example 4. *For the following highly oscillatory logarithmic-algebraic singular integral*

$$I[f(\alpha,\beta,1)] = \int_{-1}^{1} \frac{\ln(x-a)\ln(b-x)f(x)e^{i\omega x}}{(x-a)^{0.2}(b-x)^{0.3}(x-0.5)^{\gamma}}dx, \tag{4.4}$$

Table 6 presents the absolute error for $f(x) = sin(x)$ and $\gamma = 1$. This shows that accurate results can be obtained for different values of N and ω. Figure 4 reveals the absolute error, while Figure 5 presents the scaled absolute error for (4.4) for different values of N and ω from 10 *to* 1000*. Figure 4 indicates that the absolute error improves as ω increases.*

Table 6. The absolute error for the integral (4.4), where $f(x) = sin(x)$ and $\gamma = 1$.

ω	N=1	N=2	N=3	N=4	N=5
16	5.9832×10^{-03}	2.2868×10^{-04}	1.9090×10^{-05}	2.2837×10^{-06}	3.5432×10^{-07}
32	1.9802×10^{-03}	2.0992×10^{-05}	5.9049×10^{-07}	2.6973×10^{-08}	1.7555×10^{-09}
64	6.5030×10^{-04}	1.7242×10^{-06}	1.3336×10^{-08}	1.8053×10^{-10}	3.7305×10^{-12}
100	2.2692×10^{-04}	3.3430×10^{-07}	1.0928×10^{-09}	6.2868×10^{-12}	5.6206×10^{-14}

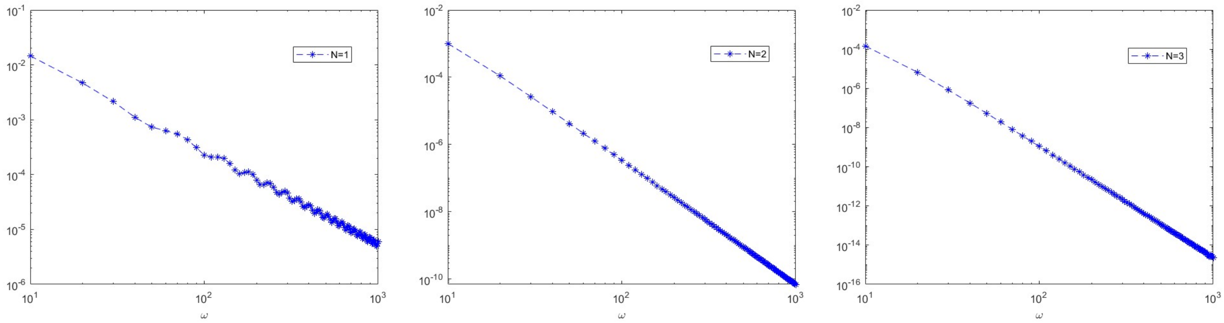

Figure 4. Absolute error for the integral (4.4), where $f(x) = sin(x)$ and $N = 1, 2, 3$.

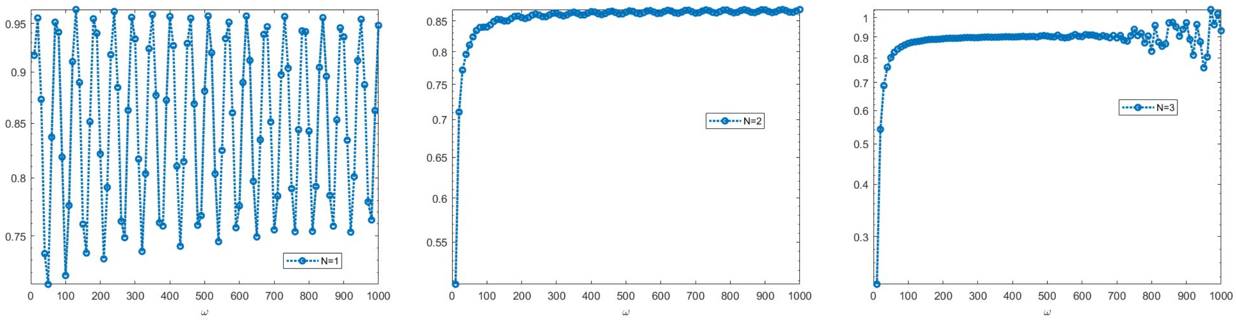

Figure 5. Absolute error scaled by (3.1) for the integral (4.4), where $f(x) = sin(x)$ and $N = 1, 2, 3$.

Example 5. *Let's consider the highly oscillatory logarithmic-algebraic singular integral as*

$$I[f(\alpha,\beta,1)] = \int_0^2 \frac{\ln(x-a)\ln(b-x)f(x)e^{i\omega x}}{(x-a)^{0.2}(b-x)^{0.4}(x-1.5)^{\gamma}}dx. \tag{4.5}$$

Table 7 gives the absolute error results for $f(x) = cos(x)$ and $\gamma = 0$. Figures 6 and 7 reveal the absolute error and scaled absolute error of (4.5) for different values of N and ω from 10 *to* 1000*, respectively. Figure 6 presents an improvement in absolute error for higher values of ω.*

Table 7. The absolute error for the integral (4.5), where $f(x) = cos(x)$ and $\gamma = 0$.

ω	N=1	N=2	N=3	N=4	N=5
16	7.7189×10^{-03}	3.3414×10^{-05}	2.7082×10^{-08}	1.9848×10^{-10}	6.9663×10^{-12}
32	2.7662×10^{-03}	3.1279×10^{-06}	2.7699×10^{-10}	2.3940×10^{-12}	6.3064×10^{-15}
64	9.5127×10^{-04}	2.7529×10^{-07}	2.2501×10^{-12}	1.8275×10^{-14}	5.1516×10^{-16}
100	3.3617×10^{-04}	4.2396×10^{-08}	9.7764×10^{-13}	4.9183×10^{-16}	3.8560×10^{-16}

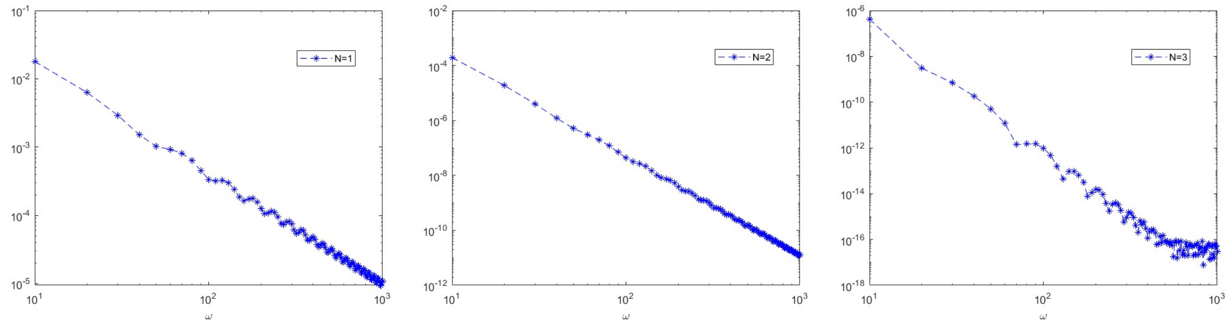

Figure 6. Absolute error for the integral (4.5), where $f(x) = cos(x)$ and $N = 1, 2, 3$.

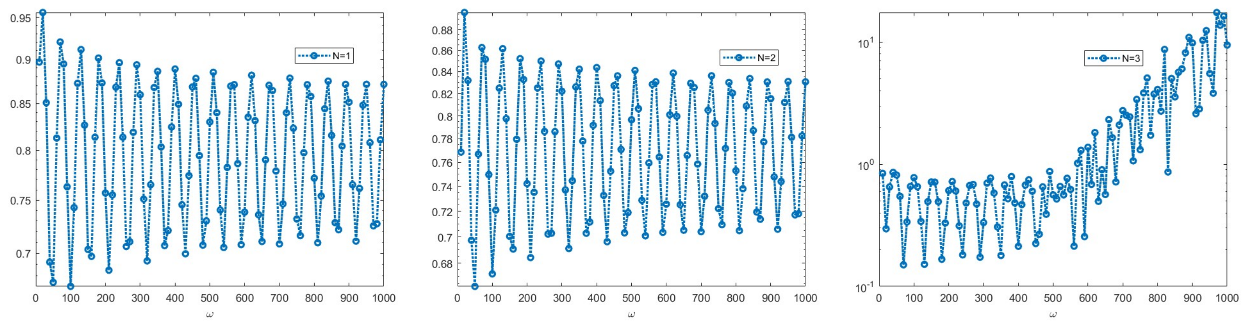

Figure 7. Absolute error scaled by (3.1) for the integral (4.5), where $f(x) = cos(x)$ and $N = 1, 2, 3$.

Example 6. *Let's consider the following highly oscillatory logarithmic-algebraic singular integral as*

$$I[f(\alpha,\beta,0)] = \int_0^1 \frac{[\ln(x-a)\ln(b-x)]^s f(x)e^{i\omega x}}{(x)^{0.5}(1-x)^{0.34}}dx. \tag{4.6}$$

Table 8 represents the comparison of absolute and relative errors given in [14] for (4.6) for $f(x) = cos(x)$ and $s = \gamma_k = 0$. The proposed method can obtain more accurate results for $N = 5$ than the Clenshaw-Curtis-Filon method discussed in [14].

Table 8. The comparison for the integral (4.6), where $f(x) = cos(x)$ and $s = \gamma_k = 0$ with [14].

ω	AE_5 [14]	$AE_5[f(\alpha,\beta,0)]$	RE_5 [14]	$RE_5[f(\alpha,\beta,0)]$
500	4.7×10^{-9}	4.7×10^{-15}	6.1×10^{-8}	6.0×10^{-14}
1000	9.4×10^{-10}	3.6×10^{-15}	1.5×10^{-8}	5.9×10^{-14}
3000	1.1×10^{-10}	2.3×10^{-15}	3.1×10^{-9}	6.7×10^{-14}
5000	7.7×10^{-11}	3.1×10^{-15}	3.4×10^{-9}	1.4×10^{-13}

Table 9 illustrates the absolute error comparison for (4.6) for $f(x) = sin(x)$, $s = 1$, and $\gamma_k = 0$ with results provided in [19]. The proposed method obtains high precision results as ω increases compared to the high order Clenshaw-Curtis-Filon method based on Hermite interpolation $P_{N+2r}, r = 0, 1, 2$ discussed in [19].

Table 9. The comparison for integral (4.6), where $f(x) = sin(x)$, $s = 1$, and $\gamma_k = 0$ with [19].

w		25		100		400	
N	r	$AE_N[I^{HCCF}][19]$	$AE_N[f(\alpha,\beta,1)]$	$AE_N[I^{HCCF}][19]$	$AE_N[f(\alpha,\beta,1)]$	$AE_N[I^{HCCF}][19]$	$AE_N[f(\alpha,\beta,1)]$
	0	4.2×10^{-03}		3.7×10^{-04}		7.4×10^{-05}	
2	1	2.5×10^{-06}	2.5×10^{-05}	7.8×10^{-08}	3.2×10^{-09}	9.6×10^{-10}	3.6×10^{-12}
	2	3.1×10^{-09}		5.7×10^{-10}		6.4×10^{-12}	
	0	6.8×10^{-05}		4.4×10^{-06}		8.0×10^{-07}	
4	1	6.5×10^{-08}	3.2×10^{-09}	5.4×10^{-10}	1.1×10^{-13}	7.7×10^{-11}	4.8×10^{-16}
	2	7.3×10^{-11}		8.2×10^{-13}		5.8×10^{-14}	
	0	2.1×10^{-08}		8.7×10^{-09}		1.9×10^{-09}	
6	1	5.0×10^{-11}	3.6×10^{-12}	6.9×10^{-12}	4.8×10^{-16}	5.3×10^{-14}	3.2×10^{-16}
	2	8.4×10^{-14}		1.2×10^{-14}		3.7×10^{-15}	

5. Conclusions

This paper proposes and illustrates substantiation of performance for the proposed method to compute the integral (1.1). The presented method exhibited an astonishing comparison with [14, 19] that shows higher precision approximation for N fixed as the frequency ω increased for singular integrals. Moreover, the method was found to be accurate and effective at moderate and very large frequencies. All the above figures and tables demonstrate that as ω or N increases, the current approach can produce more accurate approximations. In conclusion, the robustness and stability of the proposed method ensure its reliability for calculating highly oscillatory logarithmic-algebraic singular integrals.

Author contributions

SAIRA: Conceptualization, formal analysis, investigation, writing-original draft, writing-review & editing, supervision; Wenxiu Ma: supervision, Conceptualization, formal analysis, investigation, writing-review & editing; Suliman Khan: Conceptualization, formal analysis, writing-review & editing. All authors have read and approved the final version of the manuscript for publication.

Use of Generative-AI tools declaration

The authors declare they have not used Artificial Intelligence (AI) tools in the creation of this article.

Conflict of interest

All authors declare no conflict of interest in this paper.

References

1. D. L. Colton, R. Kress, *Inverse acoustic and electromagnetic scattering theory*, Cham: Springer, 2019. https://doi.org/10.1007/978-3-030-30351-8

2. W. X. Ma, Y. Huang, F. Wang, Inverse scattering transforms for non-local reverse-space matrix non-linear Schrödinger equations, *Eur. J. Appl. Math.*, **33** (2022), 1062–1082. http://dx.doi.org/10.1017/S0956792521000334
3. J. C. Nédélec, *Acoustic and electromagnetic equations: integral representations for harmonic problems*, 1 Ed., New York: Springer, 2001. https://doi.org/10.1007/978-1-4757-4393-7
4. E. R. Pike, P. C. Sabatier, *Scattering, two-volume set: scattering and inverse scattering in pure and applied science*, 1 Ed., New York: Academic Press, 2001.
5. G. Arfken, H. Weber, F. Harris, *Mathematical methods for physicists*, San Diego: Academic Press, 2012. https://doi.org/10.1016/C2009-0-30629-7
6. W. X. Ma, Inverse scattering and soliton solutions of nonlocal complex reverse-spacetime mKdV equations, *J. Geom. Phys.*, **157** (2020), 103845. https://doi.org/10.1016/j.geomphys.2020.103845
7. W. X. Ma, Riemann-Hilbert problems and soliton solutions of a multicomponent mKdV system and its reduction, *Math. Method. Appl. Sci.*, **42** (2019), 1099–1113. https://doi.org/10.1002/mma.5416
8. L. Cheng, Y. Zhang, W. X. Ma, An extended (2 + 1)-dimensional modified Korteweg-de Vries-Calogero-Bogoyavlenskii-Schiff equation: Lax pair and Darboux transformation, *Commun. Theor. Phys.*, **77** (2025), 035002. https://doi.org/10.1088/1572-9494/ad84d3
9. S. Xiang, Efficient Filon-type methods for $\int_a^b f(x)e^{\iota\omega g(x)}dx$, *Numer. Math.*, **105** (2007), 633–658. https://doi.org/10.1007/s00211-006-0051-0
10. E. A. Flinn, A modification of Filon's method of numerical integration, *J. ACM*, **7** (1960), 181–184. https://doi.org/10.1145/321021.32102
11. S. Olver, Moment-free numerical integration of highly oscillatory functions, *IMA J. Numer. Anal.*, **26** (2006), 213–227. https://doi.org/10.1093/imanum/dri040
12. S. Khan, S. Zaman, A. Arama, M. Arshad, On the evaluation of highly oscillatory integrals with high frequency, *Eng. Anal. Bound. Elem.*, **121** (2020), 116–125. https://doi.org/10.1016/j.enganabound.2020.09.010
13. C. W. Clenshaw, A. R. Curtis, A method for numerical integration on an automatic computer, *Numer. Math.*, **2** (1960), 197–205. https://doi.org/10.1007/BF01386223
14. H. Kang, S. Xiang, Efficient integration for a class of highly oscillatory integrals, *Appl. Math. Comput.*, **218** (2011), 3553–3564. https://doi.org/10.1016/j.amc.2011.08.101
15. D. Huybrechs, S. Vandewalle, On the evaluation of highly oscillatory integrals by analytic continuation, *SIAM J. Numer. Anal.*, **44** (2006), 1026–1048. https://doi.org/10.1137/050636814
16. H. Kang, R. Wang, M. Zhang, S. Xiang, Efficient and accurate quadrature methods of Fourier integrals with a special oscillator and weak singularities, *Appl. Math. Comput.*, **440** (2023), 127492. https://doi.org/10.1016/j.amc.2022.127492
17. C. Fang, Efficient methods for highly oscillatory integrals with weak and Cauchy singularities, *Int. J. Comput. Math.*, **93** (2016), 1597–610. https://doi.org/10.1080/00207160.2015.1067312
18. S. Khan, S. Zaman, Siraj-ul-islam, Approximation of Cauchy-type singular integrals with high frequency Fourier kernel, *Eng. Anal. Bound. Elem.*, **130** (2021), 209–219. https://doi.org/10.1016/j.enganabound.2021.05.017
19. H. Kang, C. Ling, Computation of integrals with oscillatory singular factors of algebraic and logarithmic type, *J. Comput. Appl. Math.*, **285** (2015), 72–85. https://doi.org/10.1016/j.cam.2015.02.006

20. A. Arama, S. Xiang, S. Khan, On the convergence rate of Clenshaw-Curtis quadrature for Jacobi weight applied to functions with algebraic endpoint singularities, *Symmetry*, **12** (2020), 716. https://doi.org/10.3390/sym12050716
21. G. He, S. Xiang, An improved algorithm for the evaluation of Cauchy principal value integrals of oscillatory functions and its application, *J. Comput. Appl. Math.*, **280** (2015), 1–13. https://doi.org/10.1016/j.cam.2014.11.023
22. A. Hascelik, Efficient computation of highly oscillatory Fourier-type integrals with monomial phase functions and Jacobi-type singularities, *Appl. Numer. Math.*, **150** (2020), 303–312. https://doi.org/10.1016/j.apnum.2019.10.007
23. R. Chen, Fast computation of a class of highly oscillatory integrals, *Appl. Math. Comput.*, **227** (2014), 494–501. https://doi.org/10.1016/j.amc.2013.11.068
24. D. K. Kurtoğlu, A. I. Hasçelik, G. V. Milovanović, A method for efficient computation of integrals with oscillatory and singular integrand, *Numer. Algor.*, **85** (2020), 1155–1173. https://doi.org/10.1007/s11075-019-00859-8
25. J. Gao, Numerical analysis of the spectrum for the highly oscillatory integral equation with weak singularity, *J. Comput. Appl. Math.*, **403** (2022), 113820. https://doi.org/10.1016/j.cam.2021.113820
26. Y. Wang, S. Xiang, Fast and stable augmented Levin methods for highly oscillatory and singular integrals, *Math. Comp.*, **91** (2022), 1893–1923. https://doi.org/10.1090/mcom/3725
27. S. Lang, *Complex analysis*, 4 Eds., New York: Springer, 1998. https://doi.org/10.1007/978-1-4757-3083-8
28. W. Gautschi, Gauss quadrature routines for two classes of logarithmic weight functions, *Numer. Algor.*, **55** (2010), 265–277. https://doi.org/10.1007/s11075-010-9366-0
29. P. J. Davis, P. Rabinowitz, *Methods of numerical integration*, New York: Academic Press, 1984. https://doi.org/10.1016/C2013-0-10566-1
30. J. S. Ball, N. H. Beebe, Efficient Gauss-related quadrature for two classes of logarithmic weight functions, *ACM Trans. Math. Softw.*, **33** (2007), 19. https://doi.org/10.1145/1268769.1268773